IOPscience iopscience.iop.org

Home Search Collections Journals About Contact us My IOPscience

Anomalous magnetoresistance peaks in quantum Hall plateau regions

This article has been downloaded from IOPscience. Please scroll down to see the full text article.

1995 J. Phys.: Condens. Matter 7 4517

(http://iopscience.iop.org/0953-8984/7/23/020)

View the table of contents for this issue, or go to the journal homepage for more

Download details:
IP Address: 171.66.16.151
The article was downloaded on 12/05/2010 at 21:27

Please note that terms and conditions apply.

J. Phys.: Condens. Matter 7 (1995) 4517–4523. Printed in the UK

Anomalous magnetoresistance peaks in quantum Hall plateau regions

S K Noh†, J I Lee†, G Ihm‡, J H Oh§ and K J Chang§

† Epitaxial Semiconductor Group, Korea Research Institute of Standards and Science, Taejon 305-606, Korea

‡ Department of Physics, Chungnam National University, Taejon 305-764, Korea

§ Department of Physics, Korea Advanced Institute of Science and Technology, Taejon 305-338, Korea

Received 19 December 1994, in final form 14 March 1995

Abstract. We find anomalous magnetoresistance peaks in a narrow Hall conductor, which are positioned in the quantum Hall plateau regions rather than in the plateau transition regions. Such peculiar behaviour can be explained quantitatively by using a model based on the edge current picture, in which the Landau levels crossing the Fermi energy are different in the conducting segments of the current and voltage probes of the sample. The Landau level offset is attributed to the non-uniform distribution of the carrier density.

Studies of the quantum Hall effect (QHE) in a narrow Hall conductor have attracted much attention recently. Of special interest in searching for the QHE breakdown mechanism is the interrelationship between the Hall resistance (R_{xy}) and the concurrent longitudinal resistance (R_{xx}) [1–5]. It is well known that the QHE is characterized by a series of plateaus in R_{xy} sweeping the magnetic field applied to a two-dimensional electron gas (2DEG), with the minima of the Shubnikov–de Haas (SdH) oscillations of R_{xx} at the plateaus [6]. In a plateau transition region, R_{xy} varies smoothly with magnetic field from one quantized value to the other, while R_{xx} exhibits a peak.

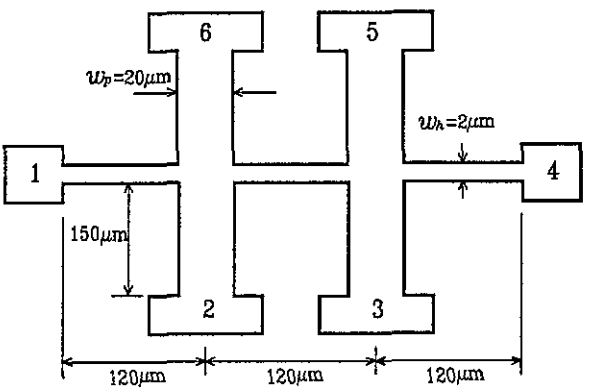

Figure 1. A schematic view of the sample geometry for the narrow-bar device.

In this paper we report a contradictory case to the usual QHE, which is observed in a narrow Hall conductor. In the Hall bar geometry given in figure 1, we find some peaks

in R_{xx} at the plateaus, while in the usual QHE these peaks appear in the transition regions between the plateaus. However, the minima of R_{xx} are still located at the plateaus. Using the edge state model [7, 8] with a constraint that the Landau level crossings of the Fermi level in the conducting segments of the current and voltage probes are different, we are able to explain quantitatively the anomalous feature observed in the QHE effect. The Landau level offset at the Fermi level is attributed to the inhomogeneous distribution of the 2D carrier density in the Hall bar, and this is confirmed by experiments. This situation is similar to the previous observations [10] on a sample consisting of a gated Hall bar geometry in which the carrier concentration in the gate region was controlled in a systematic way and the noticeable anomaly in the longitudinal resistance was found. The edge state picture has been successful in explaining unusual conducting behaviour of the 2D electron gas, such as the dramatic nonlocal effect on the multi-terminal resistance [9] and the gated-region transport of a Hall conductor in the QH regime [10]. In this model, the role of each conducting segment in the Hall device was shown to be important and its importance is also demonstrated in the present work. Since in our sample the width ($w_p = 20$ μm) of the conducting segment in the voltage probe is much larger than that ($w_h = 2$ μm) of the narrow Hall bar, the plateau transitions in R_{xy} are mainly determined by the properties of the voltage probe. Thus, despite the presence of inter- and intra-channel backscatterings in the narrow Hall bar, the QHE exhibits distinct plateaus in R_{xy}.

The QH devices were fabricated by the standard photolithographic technique from high-mobility GaAs/AlGaAs heterojunction materials, with a nominal two-dimensional density of 3.9×10^{11} cm^{-2} and a mobility of 5×10^5 cm^2 V^{-1} s^{-1}, both measured at 1.5 K. The current applied to the Hall device was fixed at 0.1 μA.

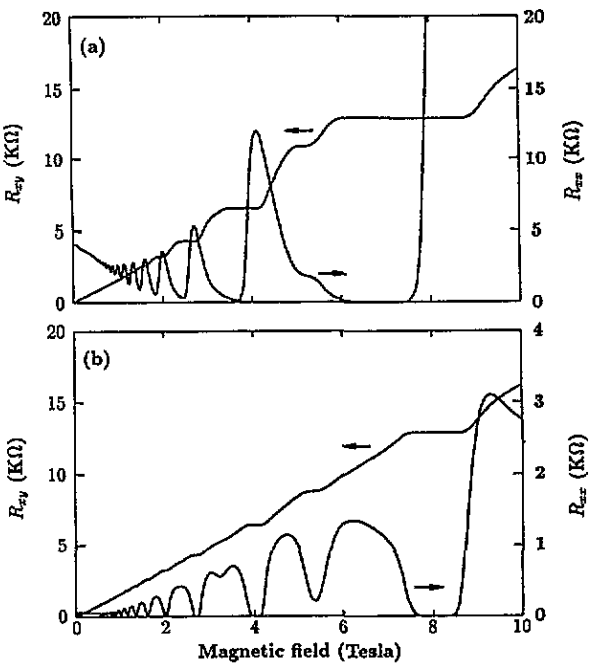

Figure 2. R_{xy} and R_{xx} are plotted as a function of magnetic field for the Hall devices with (a) $w_h = 2$ μm (shown in figure 1) and (b) $w_h = 65$ μm.

For the Hall device with a narrow conducting channel width of $w_h = 2$ μm, the

magnetic field dependences of the Hall resistance (R_{xy}) and the longitudinal resistance (R_{xx}) are plotted in figure 2(a), and both the QH plateaus and SdH oscillations are clearly observed. However, we find anomalous peaks in the SdH oscillation at the plateaus. We also test the other sample with a larger channel width, $w_h = 65$ μm, fabricated from the same heterostructure wafer, and find the normal SdH oscillations with the peaks located in the plateau transition region as shown in figure 2(b). To get more information on the narrow-bar sample, we perform resistance measurements for the Hall bar geometry in figure 1. If we define $R_{ij,kl}$ as the resistance between the probes k and l with the current flowing from the probe i to j, we find that $R_{62,14}$ is equal to the Hall resistance R_{xy} in figure 2(a), i.e., $R_{14,26}$ or $R_{14,35}$, while $R_{62,35} = 0$.

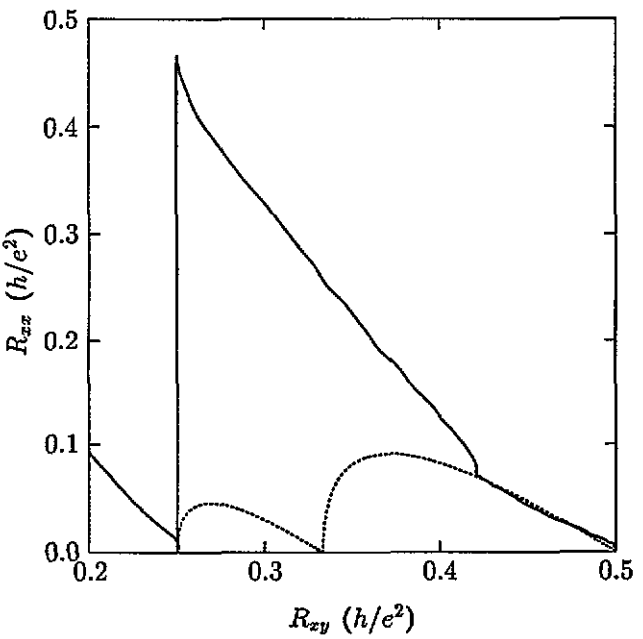

Figure 3. The measured R_{xx} versus R_{xy} relation (solid line) is plotted for the $\nu = 3$ and 4 oscillations and compared with the model calculation (dotted line) from [9].

To understand the peculiar experimental results, we first apply the theoretical model proposed by McEuen and co-workers [9], which treats separately the edge and bulk conducting pathways. This model neglects inter-channel scatterings and only considers the backscattering of the topmost Nth channel. The transmission probability t_j of the topmost channel in the conducting segment j is expressed as the ratio of length to width of the jth segment and an adjustable parameter. This model takes advantage of the ease of assessing the relationship between R_{xy} and R_{xx} with a single parameter. In figure 3, the R_{xx} versus R_{xy} relation measured for the narrow Hall bar is plotted for magnetic fields ranging from 2.9 to 6.3 T, corresponding to the $N = 3$ and 4 Landau levels, and compared with the prediction from the model proposed by McEuen and co-workers. We find significant discrepancies between theory and experiment; in the experiments the Landau levels seem to be nearly spin degenerate because the spin-up and spin-down states cannot be resolved, while the model calculations show a clear distinction between these two states. Thus, we expect the degenerate spin states, which induce the Nth and $(N-1)$th channels, to be simultaneously backscattered. However, with the degenerate spin states taken into account,

the theoretical model cannot explain a sharp sawtooth-like shape observed in experiments; the measured R_{xx}s are much larger than those calculated from the model, implying that the inter-channel tunnellings cannot be negligible. The sharp sawtooth-like shape is caused by the anomalous peak positions in R_{xx} and can be explained by imposing the condition that the Landau levels crossing the Fermi energy be different in the conducting segments of the voltage and current probes. This Landau level offset can occur either if the average electron densities are different in the two probe regions [10] or if the hybrid effect is significant between magnetic and electric confinements in the narrow-bar region [11]. With the inclusion of the depletion layer [12], the effective conducting channel width of 1.4 μm is still larger than the magnetic length of $l_c = \sqrt{\hbar/eB} \sim 10$ nm for magnetic fields considered here. Thus, the hybrid effect is expected to be too small to cause the Landau level offset at the Fermi level. In the former case, we measure the sheet carrier density of the narrow-bar sample ($w_h = 2$ μm) by two methods; the carrier density estimated from the periodicity of the SdH oscillations, which represents the average sheet carrier density in the narrow-bar region as long as the edge current picture holds, is found to be 3.66×10^{11} cm^{-2}, while the low-field Hall measurement at $B = 0.5$ T, which reflects the average density over the whole sample, gives the density of $n = 3.90 \times 10^{11}$ cm^{-2}. When we test the other sample with the channel width $w_h = 65$ μm, in which no anomalous behaviour is seen in R_{xx}, the same carrier density of 3.90×10^{11} cm^{-2} is obtained in both the measurements. Thus, because of the non-uniform distribution of the carrier density in the narrow-bar sample, we believe that the Landau level offset occurs between the two probe regions, and both the inter- and intra-channel backscatterings are enhanced.

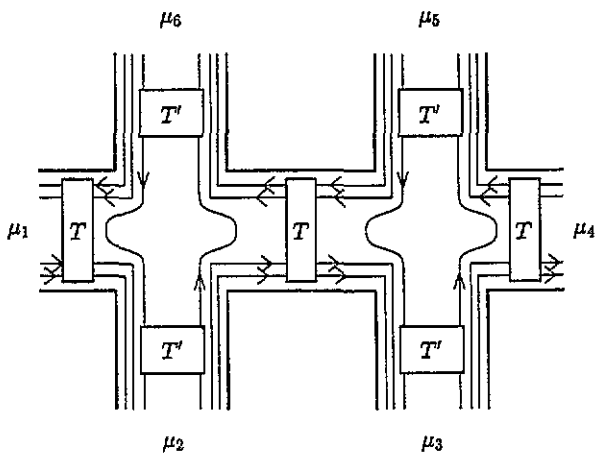

Figure 4. The current trajectories are drawn in the present model for the narrow-bar sample. T and T' denote the total transmission probabilities in the current and voltage probe regions, respectively.

Here we develop a theoretical model to explain quantitatively our experimental results in the QH regime. The current trajectories in the model are shown schematically in figure 4. The conducting segments in the narrow Hall bar have the same width and length and each segment is modelled by a barrier with the total transmission probability T, which includes inter- and intra-channel backscatterings. If the Landau level offset occurs near the Fermi energy, since the numbers of channels in the current and voltage probes, M and N, respectively, depend on the magnetic field, M can be different from N. If $N > M$, excess $(N-M)$ channels in the voltage probe are prohibited from being scattered into the

current probe but can be backscattered or scattered into the other probe on the opposite side through the barrier with the total transmission probability T'. Although the present model is quite simple, it provides important and fundamental physics for understanding the anomalous behaviour of R_{xx} without any adjustable parameters. From the multichannel and multiprobe Landauer resistance formula [8], the current I_i from the probe i is expressed as

$$I_i = \frac{e}{h}\left((\nu_i - R_{i,i})\mu_i - \sum_{j\neq i} T_{i,j}\mu_j\right) \tag{1}$$

where ν_i and μ_i represent the number of channels and the chemical potential at the probe i, respectively, and $T_{i,j}$ (or $R_{i,i}$) is the total probability for carriers incident from probe j (i) to be transmitted (reflected) to probe i. Applying equation (1) for all the six probes in figure 4 and solving for the μ_i, the magnetoresistances R_{xx} and R_{xy} can be written as

$$R_{xx} = \frac{\mu_2 - \mu_3}{eI} = \frac{h}{e^2}\frac{1}{T} - R_{xy} \tag{2}$$

$$R_{xy} = \frac{h}{e^2}\frac{1}{M + T''} \tag{3}$$

where $T'' = T'/(2 - T')$. It is interesting to note that within the present model the Hall resistance R_{xy} is independent of the transmission probability T, as illustrated in equation (3). This result implies that the plateaus of R_{xy} are mainly determined by the properties of the conducting segments of the voltage probe rather than of those in the current probe. However, the longitudinal resistance R_{xx} depends on both the probabilities, T and T'. The transmission probability T is obtained from our experimental data through the present model, equations (2) and (3), and is plotted with R_{xx} and R_{xy} in figure 5. The Landau level crossings at the Fermi level are also drawn schematically in the current and voltage probe regions. For the magnetic field corresponding to the plateau region with the filling factor $\nu = 4$ and $R_{xx} = 0$ (see the field marked by i in figure 5(a)), the Fermi level is higher than the bulk Landau level; then, R_{xy} is quantized in $h/4e^2$, and ideal edge states ($M = N = T = 4$, $T' = 0$) are formed because of there being no backscattering. As B increases to the point ii, R_{xx} increases very rapidly and reaches a maximum because the inter- and intra-channel backscatterings are dominant ($1 < T < 2$). Then, the Fermi level lies in the middle of the topmost (spin-degenerate) bulk Landau level in the current probe region, as indicated by the line ii as in figure 5(b). However, since the Landau level in the voltage probe still remains as the edge state ($M = N = 4$, $T' = 0$), a plateau still shows up in R_{xy}. This result is consistent with experimental observations. With the further increase of B, the bulk Landau levels of the voltage probe region increase and cross the Fermi level as shown by the line iii in figure 5(c), while the topmost Landau level in the current probe is almost depleted and T approaches 2. In this case, R_{xy} undergoes the plateau transition and backscatterings ($T' \neq 0$) begin to contribute. We should point out that although R_{xy} exhibits some flattening for a magnetic field marked by iv in figure 5(a), this does not correspond to the $\nu = 3$ plateau, but is caused by the spin splitting. In the 2D electron gas under magnetic fields, the spin-splitting energy ΔE is larger than its bulk value, $\Delta E^{\text{bulk}} = g_0\mu_B B$, because of the electron exchange effect [12]:

$$\Delta E = g^*\mu_B B = g_0\mu_B B + E_{ex}^0(n_\uparrow - n_\downarrow) \tag{4}$$

where μ_B and g_0 denote the Bohr magneton and the Landé g-factor of a free electron, respectively, and $n_\uparrow$ ($n_\downarrow$) is the relative number of spin-up (spin-down) electrons. As the upper spin state is depopulated, the spin-splitting energy increases, resulting in the reduction

of backscattering. The effect of the spin splitting on R_{xy} was also observed in previous work by Richter and co-workers [14]; however, an overshoot of R_{xy} was demonstrated instead of the flattening.

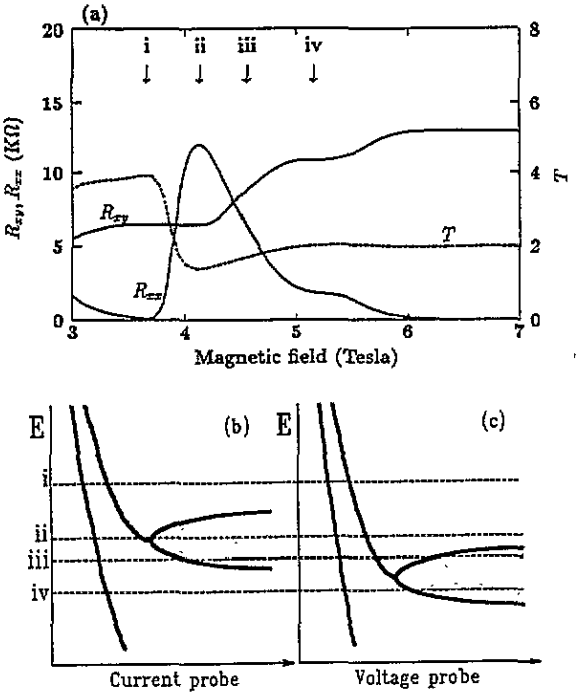

Figure 5. In (a), R_{xx}, R_{xy}, and T (defined in figure 4) are plotted as a function of magnetic field. The spin-degenerate Landau levels are drawn schematically near the edges of the conducting segments in the (b) current and (c) voltage probes. Solid lines denote edge states while the bulk Landau levels are given by shaded areas. The Fermi levels relative to the Landau levels are represented by dashed lines for the magnetic fields specified in (a).

To confirm our model for the anomalous behaviour of R_{xx}, we performed resistance measurements by switching probes in the sample; with the current flowing from probe 6 to probe 2, the resistances, $R_{62,14}$ and $R_{62,35}$, between the probes 1 and 4 and between the probes 3 and 5, respectively, were measured. Unexpectedly, we find that $R_{62,14}$ is exactly the same as R_{xy} in figure 2, i.e., $R_{14,26}$ or $R_{14,35}$, while $R_{62,35}$ is always zero. With the present model applying for this case, the chemical potentials in the probes have the following relations: $\mu_2 = \mu_3 = \mu_4 = \mu_5$ and $\mu_1 = \mu_6 = \mu_4 + hI/e(M + T'')$. Thus, we get the results for the resistances, which are consistent with experiments:

$$R_{62,14} = \frac{\mu_1 - \mu_4}{eI} = \frac{h}{e^2(M + T'')} = R_{14,26} \tag{5}$$

$$R_{62,35} = 0. \tag{6}$$

Finally, we mention that despite the successful interpretations of experimental data, the present model cannot provide a clear answer to the question of what causes the inhomogeneous distribution of the 2D carrier density throughout the narrow-bar sample. At this point, we guess that it may be caused by the specific sample geometry used in experiments. With moderate currents of about 0.1 μA supplied in the Hall bar, the Hall

fields and the electron heating may not be neglected. Furthermore, the lithographing process [15] may affect the electron density distribution because the bar width of $w_b = 2$ μm is very close to the limit of current lithographic techniques.

In conclusion we have observed the anomalous SdH oscillations in the narrow Hall conductor: some of the peaks in the longitudinal resistance appear in the quantized plateau regions. We are able to explain both quantitatively and qualitatively such peculiar behaviour using a theoretical model based on the edge current picture, where the inter-edge-state tunnelling and backscattering are enhanced because of the inhomogeneous distribution of the 2D electron density. In our specific sample geometry, the distinct QH plateaus still exist because the plateau transition is mainly governed by the conducting segments of the voltage probe rather than those in the current probe region. This demonstrates the importance of probe geometry in the QHE.

Acknowledgments

The authors are indebted to Dr K H Yoo for many valuable discussions. This work was supported in part by the SPRC of Jeonbuk National University, by the ministry of Science and Technology, Korea, and by the CMS of Korea Advanced Institute of Science and Technology.

References

[1] Kirtley J R, Schlesinger Z, Theis T N, Millikan F P, Wright S L and Palmateer L F 1986 *Phys. Rev.* B **34** 5414
[2] de Vegvar P G N, Chang A M, Timp G, Mankiewich P M, Cunningham J E, Behringer R and Howard R E 1987 *Phys. Rev.* B **36** 9366
[3] Molenkamp L W, Brugmans M J P, van Houten H, Beenakker C W J and Foxon C T 1991 *Phys. Rev.* B **43** 12 118
[4] Kent A J, Mckitterick D J, Challis L J, Hawker P, Mellor C J and Henini M 1992 *Phys. Rev. Lett.* **69** 1684
Shashkin A A, Kent A J, Harrison P A, Eaves L and Henini M 1994 *Phys. Rev.* B **49** 5379
[5] Chklovskii D B and Lee P A 1993 *Phys. Rev.* B **48** 18 060
[6] See, e.g.
Prange R E and Girvin S M (ed) 1990 *The Quantum Hall Effect* 2nd edn (Berlin: Springer)
[7] Streda P, Kucera J and MacDonald A H 1987 *Phys. Rev. Lett.* **59** 1973
[8] Büttiker M 1986 *Phys. Rev. Lett.* **57** 1761; 1988 *Phys. Rev.* B **38** 9375
[9] McEuen P L, Szafer A, Richter C A, Alphenaar B W, Jain J K, Stone A D, Wheeler R G and Sacks R N 1990 *Phys. Rev. Lett.* **64** 2062
[10] Haug R J, MacDonald A H, Streda P and von Klitzing K 1988 *Phys. Rev. Lett.* **61** 2797
Müller G, Weiss D, Koch S, von Klitzing K, Nickel H, Schlapp W and Lösch R 1990 *Phys. Rev.* B **42** 7633
Ryan J M, Deutscher N F and Ferry D K 1993 *Phys. Rev.* B **48** 8840
[11] Berggren K F, Ross G and van Houten H 1988 *Phys. Rev.* B **37** 10 118
[12] The depletion layer width is estimated by following the method described in
Choi K K, Tsui D C and Alavi K 1987 *Appl. Phys. Lett.* **50** 110
[13] Ando T and Uemera Y 1974 *J. Phys. Soc. Japan* **37** 1004
Nicholas R J, Haug R J, von Klitzing K and Weimann G 1988 *Phys. Rev.* B **37** 1294
[14] Richter C A, Wheeler R G and Sacks R N 1992 *Surf. Sci.* **263** 270
[15] Takagaki Y, Gamo K, Namba S, Ishida S, Takaoka S and Murase K 1990 *J. Appl. Phys.* **67** 340